Proteomic characterization of the *Mycobacterium marinum*-containing vacuole in *Dictyostelium discoideum*

Aurélie Guého[1,2], Cristina Bosmani[1] and Thierry Soldati[1]*

[1]Départment de Biochimie, Faculté des Sciences, Université de Genève, Genève, Switzerland

[2]Current address: Fish Physiology and Genomics Institute, INRA, Rennes, France

*Corresponding author

ABSTRACT

Mycobacterium tuberculosis, the causative agent of tuberculosis, is able to manipulate the phagosome compartment where it resides in order to establish a permissive replicative compartment called the *Mycobacterium*-containing vacuole (MCV). *Mycobacterium marinum*, a fish pathogen and a close relative of the tuberculosis group, is also able to infect the free-living amoeba and professional phagocyte *Dictyostelium discoideum* and to manipulate its phagosome maturation. By using this host/pathogen model system, we have established an innovative procedure to isolate MCVs. This procedure allowed us to isolate *M. marinum*-MCV at 1, 3 and 6 hours post infection to study the early *M. marinum*-MCV proteome. By using isobaric labelling and mass spectrometry, we quantitatively compared the proteomic composition of those MCVs isolated at different stages of the early infection phase to understand how *M. marinum* impacts on this compartment to divert it from the normal phagosomal pathway. Furthermore, we also compare the manipulated compartment *M. marinum*-MCV to non- or less manipulated compartments containing different mycobacteria strains: the non-pathogenic *M. smegmatis*, the avirulent *M. marinum*-L1D or the attenuated *M. marinum*-RD1.

Keywords

***Dictyostelium discoideum*, *Mycobacterium marinum*, infection, host-pathogen, proteome**

INTRODUCTION

Intraphagosomal bacteria have different strategies to survive and replicate in this hostile and bactericidal phagosomal environment.

It has been shown that *Mycobacterium tuberculosis* and *Mycobacterium marinum* can arrest the maturation of the phagosome where they reside and tailor it to a replication-permissive compartment, the mycobacteria-containing vacuole or MCV. However, it is still not clear if this compartment remains an early phagosome or if it has a more complex identity. Furthermore, it is still poorly understood how the virulent mycobacteria manipulate the phagosome maturation program. To answer these questions, we decided to study the proteomic composition of the *M. marinum*-MCV in *D. discoideum* and its changes during the six first hours of infection, which we term the "manipulation phase". We also compared the proteomic composition of this manipulated compartment to the proteomic composition of MCVs containing a non-pathogenic mycobacterium (*M. smegmatis*) or an attenuated *M. marinum* (L1D), unable to fully manipulate the maturation of the phagosome where they reside.

RESULTS AND DISCUSSION

Establishment of a new procedure to isolate mycobacteria-containing vacuole

In order to study the MCV proteome, the first step of this study has been to establish an experimental strategy to isolate pure fractions of those compartments from infected *D. discoideum* cells. We decided to adapt the efficient method to isolate pure fractions of latex beads-containing phagosomes (LPCBs) described previously (Dieckmann, Gueho et

al. 2012). This method is based on the light buoyant density and flotation properties of latex beads. As a brief reminder of that generic protocole, *D. discoideum* cells are fed with latex beads, phagosome maturation is stopped at different stages and cells are mechanically broken to liberate the LBCPs, which are recovered by flotation on a sucrose gradient. Our adapted strategy (**Figure 1A**), is to float up MCVs on a sucrose gradient with the help of latex beads. For this, we established conditions to adsorb latex beads onto mycobacteria by hydrophobic interactions between the latex beads and the waxy surface of the mycobacteria. The conditions used are based on a standard protocol used to adsorb proteins on latex beads. After several washing steps of both latex beads and mycobacteria in borate buffer, beads and mycobacteria were mixed and incubated on a rotating wheel. After 2 h, we could observe the formation of bacteria and beads complexes (BBCs) (**Figure 1B, and S1B**).

Different bead sizes (0.8 µm, 0.5 µm and 0.2 µm), and different bead:bacteria ratios were tested. The ratios were adapted according to the bead size: 2 and 15 for 0.8 µm beads, 30 and 90 for 0.5 µm beads, and 100 and 500 for 0.2 µm beads (**Figure S1A**). Interestingly, the highest ratios had an "individualizing" effect on the mycobacteria, as they prevented mycobacteria from sticking to each other, and allowed the formation of BBCs containing single bacteria. The BBCs obtained with 0.8 µm beads were large, about twice the size of a single mycobacteria, while 0.5 µm and 0.2 µm beads did not increase drastically the size of mycobacteria.

In order to completely cover mycobacteria with beads, a large excess of latex beads has to be used, resulting in a profusion of free beads. To isolate fractions of pure MCVs without contamination of phagosomes containing the free beads, unadsorbed beads have to be removed from the BBC preparation before infecting cells. To achieve this, a one-step sucrose gradient was sufficient (**Figure S1C**). After ultracentrifugation, BBCs could be collected at the 20% -60% sucrose interphase, whereas free beads floated up at the 20% sucrose-medium interphase.

To confirm the possibility to use BBCs to isolate MCVs, the flotation property of BBCs on the standard sucrose gradients used to isolate LBCPs was monitored (**Figure S1D**). Most of the BBCs concentrated at the 10%-25% sucrose interphase, like the LBCPs. Only few BBCs, probably with a lower ratio of beads and too dense to float to the top of the gradient, were observed at the other interphases. To increase the yield of MCV isolation, the sucrose gradient used for LBCPs (10%, 25%, 35%, 60%) was adjusted to 10%, 30%, 40%, 60%. These pilot experiments allowed us to prepare BBC inoculates without free beads and with the property to float up on sucrose gradients similar to those used for LBCPs isolation.

BBCs are recognized and phagocytosed as mycobacteria

BBCs are slightly bigger than single mycobacteria and have an irregular shape. In order to test whether *D. discoideum* cells could phagocytose them, cells were infected with non-coated *M. marinum*-GFP or *M. marinum*-GFP BBCs prepared with three different sizes of beads. At 0.5 hpi, the percentage of infected cells was measured by flow cytometry (**Figure 1C**). All three sizes of BBCs were efficiently ingested, however, the percentage of infected cells was bead-size-dependent. The highest percentage of internalized BBCs was obtained with 0.2 µm beads. Therefore, we decided to use these BBCs for further experiments.

Mycobacteria in BBCs are totally covered with latex beads. To test whether BBCs are recognized as latex beads or as mycobacteria, immunofluorescence was performed with a cocktail of antibodies against components of the mycobacterial cell wall. Interestingly, beads covering mycobacteria and free beads incubated with mycobacteria were detected by this cocktail (**Figure 1D**). This indicates that some components of the cell wall diffuse and cover the adsorbed beads In addition, materials from the mycobacteria cell wall seem to be shed in the incubation buffer and adsorbed onto free beads. To confirm that the *M. marinum*-BBCs are recognized by *D. discoideum* as mycobacteria, and not inert beads, internalization of BBCs was monitored in *lmpB*-ko cells, which are specifically defective for the uptake of mycobacteria (Sattler, Bosmani et al. 2018). As for non-coated *M. marinum*, *M. marinum*-BBCs ingestion was significantly impaired in *lmpB*-ko cells (**Figure 1E**). These results suggest that BBCs are recognized as mycobacteria

Several hours after uptake by *D. discoideum* cells, *M. marinum*-BBCs were observed in intracellular closed compartments (**Figure1G**), which were positive for p80 and vacuolin (**Figure 1F**), known markers of the MCV (Hagedorn and Soldati 2007). Latex beads could also be observed inside these compartments, indicating that mycobacteria and latex beads remain in the same compartment even several hours post-infection. Overall, our results show that BBCs are recognized and taken up as free mycobacteria, and reside in compartments similar to MCVs.

Mycobacteria in the BBCs are still alive and infectious

During preparation of BBCs, mycobacteria are subjected to different mechanical, osmotic and chemical stresses. To test whether this has an impact on the infectivity of mycobacteria, *D. discoideum* cells were infected with different non-coated GFP-expressing mycobacteria or BBCs prepared with different strains: the virulent *M. marinum*, the avirulent *M. marinum*-L1D and the non-pathogenic *M. smegmatis*. These strains are known to follow different fates and their infection cycles have been previously described (Hagedorn et al., 2007). The infection course of each bacteria or BBC was then monitored by flow cytometry (**Figure 2A**). As previously described, the non-pathogenic *M. smegmatis* was rapidly killed, and the population of infected cells progressively decreased until almost no infected cells were detected at 18 hours post-infection (hpi). The population of cells infected with the avirulent *M. marinum*-L1D also decreased at 6 hpi, while the population of extracellular mycobacteria increased. *M. marinum*-L1D is known to be exocytosed within few hours and re-ingested before being killed, resulting in a strong decrease of the population of infected cells and concomitant increase of extracellular mycobacteria at 18 hpi (Hagedorn and Soldati 2007). On the contrary, the virulent *M. marinum* is able to establish a successful infection, with a high proportion of infected cells remaining at 21 hpi. The infections performed with BBCs showed similar behavior. *D. discoideum* cells infected with *M. smegmatis*-BBCs or *M. marinum*-L1D-BBCs managed to cure the infection in several hours, whereas cells remained infected 21 hpi with *M. marinum*-BBCs. This indicated that the fate of the different BBCs is dependent on the mycobacteria strain used and that BBCs follow the same infection course as the mycobacteria they contain. These data also corroborate our previous results (**Figures 1F-G and 2C**) showing that *M. marinum*-BBCs remained in a compartment as late as 21 hpi, in contrast to inert particles, which are exocytosed in 1 or 2 hours (Hagedorn and Soldati 2007).

To test whether mycobacteria in the BBCs were still metabolically active and able to grow, *D. discoideum* cells were infected with BBCs prepared with luminescent *M. marinum* or non-coated *M. marinum*-lux. Growth was then followed by measuring the luminescence emitted by *M. marinum*-lux (**Figure 2B**). No intracellular growth difference was observed between *M. marinum* from BBCs and non-coated *M. marinum*, demonstrating that mycobacteria are alive in the BBCs.

It has been shown that at later stages of infection, *M. marinum* breaks its compartment to escape to the cytosol (Hagedorn and Soldati 2007, Lopez-Jimenez, Cardenal-Munoz et al. 2018). By electron microscopy, virulent *M. marinum* from BBCs were observed escaping their compartment at 21 hpi, indicating that the beads do not disturb the normal fate of *M. marinum* nor its virulence, as it is still able to damage the phagosome membrane (**Figure 2C**).

These results indicate that despite the stresses incurred by the mycobacteria during the preparation of BBCs, mycobacteria incorporated in the BBCs are still alive, infectious and virulent. Furthermore, the beads do not disturb the steps of a normal infection cycle.

Preliminary characterization of isolated MCV

We performed an initial characterization of MCVs after isolation at 1 hpi, as this was the earliest time point accessible technically. The recovered interphase contained a high number of BBCs (**Figure 3A**). Since uningested BBCs were washed away after the spinoculation, this recovered material was likely entirely BBCs-containing compartments. Very little other cellular material than BBCs was observed, indicating that the recovered BBC-containing MCVs were not significantly contaminated by other cellular organelles.

MCVs containing BBCs generated with two other mycobacteria, *M. marinum*-L1D or *M. smegmatis*, were also isolated at 1 hpi. Immunostainings were performed on the recovered material to test the presence of known markers of the MCV around BBCs (**Figure 3B**). This indicated the presence of a phagosomal membrane around the recovered BBCs and confirmed that MCVs can be isolated with this new procedure. Furthermore, the immunofluorescence revealed that at 1 hpi, some differences between the manipulated MCV of *M. marinum*, and the non-manipulated MCVs of *M. marinum*-L1D and *M. smegmatis,* could be detected. Indeed, only few *M. marinum* MCVs were positive for the two late phagosomal markers p80 and vacuolin (36% and 18% respectively), whereas about 60% of the *M. marinum*-L1D and *M. smegmatis* MCVs were positive for p80, and 53% of *M. marinum*-L1D MCVs and 27% of *M. smegmatis* MCVs were positive for vacuolin. Interestingly, 45% of the *M. marinum* MCVs were positive for the H^+-vATPase, confirming the observations of a previous study that showed that more than 50% of *M. marinum* MCVs transiently acquire the H^+-vATPase during the first hour of infection (Hagedorn and Soldati 2007). However, higher percentages of MCVs positive for H^+-vATPase

were found for *M. marinum*-L1D and *M. smegmatis*, 80% and 51% respectively. Altogether, these results indicate that already at 1 hpi, *M. marinum* has manipulated the compartment where it resides to divert it from the normal phagosome maturation process. In addition, *M. marinum* appears to reside in a compartment with some of the characteristics of an early phagosome. On the contrary, at 1 hpi, the avirulent *M. marinum*-L1D and the non-pathogenic *M. smegmatis* are in MCVs with characteristics of mature phagosomes. These results also demonstrate that, despite the beads and the potential stresses incurred by the mycobacteria during the different steps of the procedure, the identity of the isolated MCVs depends on the mycobacteria strain.

To verify the purity of the recovered MCVs, *M. marinum*-BBCs were isolated at 1hpi. The presence of markers for the endoplasmic reticulum (ER, monitored for protein disulfide-isomerase, PDI, and calreticulin) and for mitochondria (mitochondrial porin) was then evaluated by immunofluorescence (**Figure 3C**). Note that PDI and calreticulin are also detected transiently on early phagosomes (Dieckmann et al., 2012). Interestingly, a high proportion of *M. marinum*-BBCs were positive for both ER markers at 1hpi, especially PDI, confirming the early phagosome identity of the compartment where it resides. ER fragments not associated with BBCs were only rarely detected. Few BBCs were positive for mitochondrial porin. These results indicate that the new procedure established here allows the isolation of relatively pure fractions of MCVs. Overall, we demonstrated that BBCs are an appropriate and efficient tool to further characterize the MCV proteome.

M. marinum MCV proteome

Biological duplicates of MCVs containing *M. marinum*-BBCs where isolated at early times of infection: 1, 3 and 6 hpi. A comparative quantitative proteomic strategy was used to study their composition. 1606 *D. discoideum* proteins (**Table S1**) and 563 *M. marinum* proteins were identified and constitute the early MCV proteome. Among the *D. discoideum* proteins of the early MCV, 758 were also found in the phagosome proteome (Dieckmann, Gueho et al. 2012) and 875 in the macropinosome proteome (Journet, Klein et al. 2012), whereas 525 of these proteins were found to be unique to the early MCV proteome (**Figure 4A**). The high proportion of proteins in common between these different compartments indicates that the MCV, despite being manipulated by virulent mycobacteria, remains a compartment of phagosomal/endosomal-derived origin.

To identify pathways involved in the establishment of a permissive niche, proteins identified in the early MCV were manually sorted in different classes according to their function (**Figure 4B**). They have also been functionally clustered with the help of the DAVID functional annotation clustering tool (**Figure 4C** and **Table S2**). Comparison of the MCV proteome functional classification with the previously published phagosome proteome classification (Dieckmann, Gueho et al. 2012) indicated that overall, these compartments are very similar (**Figure 4B**). This again confirms that the MCV conserves some of its phagosomal identity. However, some differences could be noted. The 2 highest represented classes in the MCV were “gene transcription” and “protein biosynthesis”. Both were more represented in the MCV proteome than in the phagosome proteome. These classes of proteins are generally delivered through the autophagic pathway to phagosomes for degradation. Their high representation in the MCV proteome could indicate an accumulation of those proteins in a non-degradative phagosome, and thus reflect the manipulation of this compartment by *M. marinum*. This was confirmed by the functional clustering analysis, where the most significantly enriched categories, with the highest number of proteins, were “translation”, “ribosome biogenesis” and “rRNA processing” for GO terms, and “ribosome” and “RNA transport” for KEGG pathways. The cluster of GO terms “regulation of translational initiation”, “translational initiation” and “formation of translation preinitiation complex” was also found significantly enriched in the MCV (**Figures 4B-C**).

Two other classes were found slightly more represented in the MCV than in the phagosome proteome: “small GTPases” and “lipid metabolism”. These two classes were also found significantly enriched among the functionally clustered GO terms of the *M. marinum*-MCV proteome.

Interestingly, classes of proteins involved in “general metabolism”, “signaling”, “membrane trafficking”, “transporters”, “protein degradation”, “chaperones” and “cell defense” were less represented in the MCV than in the phagosome. All these classes are involved in or reflect the maturation of the phagosome (signaling and membrane trafficking) and in the establishment of an acidic and degradative compartment (transporters, protein degradation, cell defense). This indicates again that the MCV is a phagosome with a less degradative lumenal environment. Despite an under-representation in the MCV compared to the phagosome, these classes were also found significantly present in the functional annotation clustering analysis of the MCV proteome :

GO terms cluster "proton transport", "ATP hydrolysis coupled proton transport" and "ion transport", cluster "vesicle-mediated transport" and cluster "vesicle fusion", "vesicle docking", and KEGG pathways "oxidative phosphorylation", "phagosome" and "SNARE interactions in vesicular transport".

Early *M. marinum*-MCV maturation

Two different ratios were calculated for each of the 1606 proteins of the early *M. marinum*-MCV proteome: 3 hpi/1 hpi and 6 hpi/1 hpi. For each comparison, a significant cutoff threshold was calculated (**Table S5**). From this, 139 proteins were found differentially abundant on the *M. marinum*-MCV between 1 hpi and 3 hpi, and 146 proteins between 1 and 6 hpi. (**Table S3**). The ratios of those differentially abundant proteins were plotted on a graph (**Figure 5A**). Ratios that did not pass the cutoff threshold were noted as 1. From this graph, six different kinetic profiles could be distinguished during the first 6 hours of MCV establishment, compared to the composition at 1 hpi: proteins continuously depleted, proteins continuously accumulating, proteins transiently depleted at 3 hpi, proteins transiently accumulating at 3 hpi, proteins starting to accumulate only from 3 hpi onward, and finally, proteins starting to be depleted only from 3 hpi onward. 133 proteins were depleted from the MCV between 1 and 3 hpi, and 132 between 3 and 6 hpi, whereas only 6 proteins accumulated in the compartment between 1 and 3 hpi, and 59 between 3 and 6 hpi, indicating that the MCV is established mainly by depleting proteins compared to its composition one hour after formation. In order to identify the pathways involved in the establishment of a permissive MCV, the proteins accumulating or depleted from the compartment at the different time points were manually sorted and functionally clustered using the DAVID functional annotation clustering tool (**Figure 5B, C, D, E).** Overall, all the protein classes identified in the early MCV proteome were affected during the first 6 hours of infection (**Figure 5B**).

Protein classes the most depleted at 3 and 6 hpi were very similar. The "Gene transcription" class was the most represented. The cluster "transcription" was also among the most significantly enriched GO-terms both at 3 and 6 hpi. Proteins of this class being mainly delivered to phagosomes for degradation via the autophagic pathway, this might indicate that the MCV stops the normal phagosome maturation by preventing the fusion with any other intracellular compartments. Some other classes like "protein biosynthesis" and clusters like "RNA splicing" and "protein folding" have similar fate and were also found significantly enriched among the depleted proteins.

The classes "signaling", "membrane trafficking" and "small GTPases" were strongly depleted from the MCV. The cluster "small GTPase mediated signal transduction" was among the most significantly enriched clusters both at 3 and 6 hpi, confirming this result. The clusters "regulation of GTPase activity", "regulation of Rho protein signal transduction" and "intracellular signal transduction" were less enriched but found significantly present among the depleted clusters at 6 hpi. These classes and clusters are all involved in phagosome maturation. Their depletion from the early MCV again indicates that the maturation of this compartment and its fusion with other endosomal compartments is arrested. However, not only the fusion is blocked. Indeed, proteins involved in fission were also found in those classes (Dynamin A, Vps52, Vps53). Their depletion might prevent the removal of early phagosomal markers, a necessary step for further MCV maturation, potentially explaining how the MCV identity is reported to resemble the early phagosome stage.

The cluster "proton transport" was significantly present among the depleted proteins both at 3 and 6 hpi. The depletion of components of the V-ATPase allows to avoid or to rapidly stop the acidification of the MCV lumen.

The class "general metabolism" was depleted indicating that the entire cell metabolism could be affected during mycobacterial infection. More precisely, the "lipid metabolism" class was depleted at 3 and 6 hpi. Among those proteins were oxysterol binding proteins 8 and 12, which are involved in sterol transport. Their depletion could prevent removal of lipids from the MCV. Furthermore, from 3 hpi, this class accumulated again in the MCV. However, instead of lipid transporter, proteins really involved in lipid metabolism accumulated from 3 hpi. This would allow the mycobacteria to access and use host lipids (Barisch and Soldati 2017).

As the "lipid metabolism" class, other classes started to accumulate again from 3 hpi. Classes "protein biosynthesis" and "gene transcription" were among the most accumulating ones. Clusters "transcription" and "RNA splicing" were also significantly enriched at 6 hpi. This indicates that after preventing fusion with endo-lysosomal compartments, the MCV starts again to interact with intracellular compartments after 3 hpi. However, the accumulation of those classes of proteins indicates that the lumen of the MCV remains non-degradative and that it fuses only with non-degradative compartments. The accumulation, to a

lesser extent, of the classes "membrane trafficking" and "small GTPases" from 3 hpi confirmed this hypothesis.

It is interesting to notice that there was only one protein continuously accumulating on the MCV during the 6 first hours of infection. This protein was a phox-domain containing protein that appears to be a homolog of human Snx4. Through its association with the protein KIBRA, it is involved in the sorting of the transferrin receptor from early endosomes to the endocytic recycling compartment (ERC). Interestingly, the *D. discoideum* KIBRA homolog, a WW domain-containing protein, was also found differentially abundant during MCV establishment. However, it was continuously depleted, potentially blocking Snx4 function and further phagosome maturation, and consequently leading to the accumulation of Snx4 on the MCV.

In conclusion, 2 phases could be distinguished during the 6 first hours of MCV establishment. From 1 to 3 hpi, fusion of the MCV with endo-lysosomal compartments is blocked. Proteins involved in phagosome maturation, and in establishment of a degradative environment are removed. Fission is also blocked, preventing removal of early phagosomal markers. From 3 to 6 hpi, fusions with non-degradative intracellular compartments might be increased again. As lipid metabolism proteins start accumulating, these fusions could allow the delivery of lipids or any nutrient necessary for the growth of the mycobacteria.

M. marinum MCV comparison with non-manipulated Mycobacterium-containing compartments

Biological duplicates of MCVs containing *M. marinum*, *M. smegmatis* or *M. marinum*-RD1 were isolated at 1 and 6 hpi. MCVs containing *M. marinum*-L1D were isolated only at 1 hpi since *M. marinum*-L1D is rapidly exocytosed (Hagedorn and Soldati 2007). A comparative quantitative proteomic strategy was used to compare *M. marinum*-MCV composition to other *Mycobacteria*-MCVs at 1 and at 6 hpi. For each comparison, protein ratios were calculated. A significant cutoff threshold was calculated (**Table S5**) in order to select proteins significantly enriched or depleted on the *M. marinum*-MCV (**Table S4**). For each comparison, the number of proteins significantly enriched or depleted on the *M. marinum*-MCV is presented in **Figure 6A**.

At 1 hpi already, numerous proteins were found differentially abundant indicating that as early as at 1 hpi, *M. marinum* has diverted its compartment from the normal phagosome maturation pathway. Furthermore, the 1 hpi comparisons results reflect the different fate of the mycobacteria strains used : *M. marinum*-L1D and *M. smegmatis* are not able to manipulate their containing-vacuole and are rapidly killed and exocytosed whereas *M. marinum*-RD1, despite its lacking RD1 locus necessary to manipulate the phagosome maturation, can survive in its MCV up to 30 hours, indicating a partial manipulation of its containing-vacuole (Cardenal-Munoz, Arafah et al. 2017). Indeed, at 1 hpi, *M. marinum*-MCV in mainly depleted in proteins compared to *M. marinum*-L1D and *M. smegmatis*-MCV, whereas it is mainly enriched in proteins compared to *M. marinum*-RD1-MCV. For this reason, the comparison of M. marinum-MCV with M. marinum-RD1-MCV will be discussed later.

Not surprisingly, among the proteins less abundant on the *M. marinum*-MCV at 1 hpi were found proteins involved in intracellular bacterial killing like Phg1a and kil1 (Benghezal, Fauvarque et al. 2006, Le Coadic, Froquet et al. 2013), vATPases subunits necessary for intraphagosomal acidification (Clarke, Kohler et al. 2002), the lysosomal enzyme Cystein protease and proteins involved in membrane trafficking like annexin 7 and vps13c. Several small GTPases were also found less abundant on the *M. marinum*-MCV at 1 hpi : Sar1A, Rab14, Rab2a, an Arf GTpase, the GTPase binding protein Yip1. Small GTPases being involved in vesicular trafficking and fusion, it is not surprising that they are less abundant in the *M. marinum*-MCV, confirming its limited interaction with other intracellular compartments. Interestingly, several proteins involved in lipid metabolism were found depleted from the *M. marinum*-MCV at 1 hpi : Dgat2, Erg24, Lip5, sterol 14-demethylase, SmtA. At 1 hpi, these proteins could have been relocalised to lipid droplets in order to favour production and storage of lipids. Indeed, lipid droplets rapidly cluster around the *M. marinum*-MCV after infection. Their content is then transferred into the replicative niche (Barisch, Paschke et al. 2015).

Numerous proteins involved in gene transcription and mRNA translation were also found depleted in the *M. marinum*-MCV, indicating again its limited fusion with other intracellular compartments, and notably autophagosomes.

Among the proteins enriched on the *M. marinum*-MCV were found some cytoskeleton proteins (LimE, PirA and WH2 domain-containing protein. Two small GTPases were also found enriched et 1 hpi on the *M. marinum*-MCV: RasB and Arf1. Interestingly, Arf1, after activation by ACAP-A is involved in actin cytoskeleton remodeling. The enrichment of both cytoskeleton proteins and Arf1 confirms that the *M.*

marinum-MCV retains an actin coat to prevent delivery of vATPase (Kolonko, Geffken et al. 2014) The retromer subunit vps5 was also found enriched. Retromer throught its interaction with the WASH complex might be involved in recycling processes both at early (surface proteins) and late (mannose-6-phosphate lysosomal enzymes) macropinosome stages (Buckley, Gopaldass et al. 2016). Its enrichment on *M. marinum*-MCV at 1 hpi could either indicate a arrest of early recycling steps in order to keep early phagosomal marker and consequently, its accumulation on the MCV. It could also indicate an active retrieval of lysosomal enzymes.

At 6 hpi, we found only enriched proteins on the *M. marinum*-MCV compared with *M. smegmatis*-MCV. Numerous of these proteins were involved in gene transcription and mRNA translation. This confirms the non-degradative environment in the *M. marinum*-MCV, allowing the accumulation of protein potentially targeted to phagosome for degradation. Two proteins involved in lipid metabolism were found enriched : PLC and oxysterol binding protein 7. At this stage, it is know that lipid droplet content can be observed in the *M. marinum*-MCV (Barisch, Paschke et al. 2015). Host lipids are then used by the mycobacteria. Oxysterol binding protein 7 could be important for the transfert of lipid from the lipid droplets to the MCV. PLC would allow M. marinum to use host phospholipids as previously proposed (Barisch and Soldati 2017). Interestingly, a small GTPase, Roco5, was found accumulated in the *M. marinum*-MCV at 6 hpi.

MATERIAL AND METHODS

D. discoideum cell culture

Wild-type *D. discoideum* cells (AX2) were cultivated at 22°C in HL5c medium supplemented with 100 U/mL penicillin and 100 µg/mL streptomycin (Invitrogen). The *lmpB* ko cells were kindly provided by Dr. M. Schleicher (Janssen et al., 2001; Karakesisoglou et al., 1999).

Mycobacteria culture

Mycobacteria were cultivated at 32°C under shaking conditions (150 rpm) in Middlebrook 7H9 medium (Difco), 0.2% glycerol and 0.05% Tween 80 supplemented with 10 % OADC (Beckton Dickinson). They were cultivated in presence of 5 mm glass beads in order to avoid bacteria clumping. *M. marinum*-GFP, *M. marinum* RD1-GFP and *M. smegmatis*-GFP were cultivated in presence of 50 µg/mL kanamycin, *M. marinum* L1D-GFP in presence of 50 µg/mL apramycin and *M. marinum*-LuxABCDE in presence of 50 µL/mL hygromycin.

Preparation of bacteria+beads complexes (BBCs) inoculum

Latex beads and 5.10^9 mycobacteria were washed 3 times separately in 0.1 M borate for 10 min at 12 000 rpm, RT. The amount of latex beads to prepare was adapted according to the latex bead size: beads:bacteria ratio of 500:1 for 0.2 µm beads, 90:1 for 0.5 µm beads and 15:1 for 0.8 µm beads. After resuspension in 0.1 M borate, latex beads were sonicated for 5 min in a sonicator bath. The latex beads and the mycobacteria were then mixed and incubated on a rotating wheel for 2 h. The mycobacteria+beads mix was subsequently washed once in HL5c medium for 10 min at 12 000 rpm, and resuspended in HL5c. In order to remove unattached beads, the mix was deposited on top of a one-step sucrose gradient (20% sucrose and 60% sucrose) and ultracentrifuged for 30 min at 55 000 rpm in a TLS55 rotor. The pure inoculum of mycobacteria+beads complexes was recovered at the 20-60% sucrose interphase. It was then washed once in HL5c medium for 10 min at 12 000 rpm and finally resuspended in HL5c medium without pen/strep.

Phagocytosis assay

Phagocytosis of *M. marinum*-GFP or *M. marinum*-GFP-BBCs by AX2 and *LmpB ko* cells was monitored by FACS as previously described (Sattler et al., 2013). Briefly, cells from confluent plates were resuspended in 5 mL of fresh HL5c medium at a density of 2.10^6 cells/mL and agitated for 2 h at 150 rpm, 22°C, prior to the experiment. 2.10^8 *M. marinum*-GFP were prepared per cell line (MOI = 100). Bacteria were washed twice in HL5c medium and resuspended in 1mL of HL5c. In order to declump aggregates, mycobacteria were passaged through a 25-gauge needle for 8-10 times. 0.2 µm *M. marinum*-GFP-BBCs were prepared as described before. At T0, cells were agitated at 120 rpm and the mycobacteria or BBCs were added to the cells. At each time point, an aliquot was taken. The phagocytosis was stopped by adding one volume of ice-cold Sorensen-Sorbitol-Azide (15 mM KH_2PO_4, 2 mM Na_2HPO_4, 120 mM Sorbitol, 5 mM azide). After centrifugation 10 min at 1200 rpm at 4°C, cells were resuspended in Sorensen-Sorbitol (15 mM KH_2PO_4, 2 mM Na_2HPO_4, 120 mM sorbitol) and the fluorescence was measured by FACS. FACS measurement was performed on a FACScalibur (Beckton Dickinson) and the data analysed with FlowJo (TreeStar, USA).

Infection assay

Infections were performed as previously described (Hagedorn and Soldati 2007, Arafah, Kicka et al. 2013, Sattler, Monroy et al. 2013). *D. discoideum* cells were infected with 5.10^8 mycobacteria or 500 µL of prepared BBCs inoculum. Infections with GFP-expressing mycobacteria were monitored by FACS (Sattler, Monroy et al. 2013). At times of interest, infection aliquots were mixed V:V with Sorensen-azide (15 mM KH_2PO_4, 2 mM Na_2HPO_4, 5 mM azide) and pelleted for 4 min at 12 000 rpm, RT. The pellet was resuspended in Sorensen-Sorbitol (15 mM KH_2PO_4, 2 mM Na_2HPO_4, 120 mM sorbitol). Prior to FACS measurement, 4.5 µm fluorescent beads (100

beads/µL, YG-beads, Polyscience) were added to the sample as an internal particle concentration standard. FACS measurement was performed on a FACScalibur (Beckton Dickinson) and the data analysed with FlowJo (TreeStar, USA). Infections with bioluminescent bacteria were monitored with a plate reader (Synergy Mx, Biotek) (Arafah, Kicka et al. 2013). At times of interest, 150 µL aliquots of infected cells were deposited in a white 96-well plate (F96 MicroWell™ Plates, non-treated form Nunc) and the luminescent signal was measured with the help of the plate reader.

Immunofluorescence

D. discoideum infected cells and BBCs were fixed with PFA/picric acid or by shock-freezing fixation in -85°C methanol as described previously (Hagedorn, Neuhaus et al. 2006). The following antibodies were used: vacuolin (221-1-1, Dr. M. Maniak (Jenne, Rauchenberger et al. 1998)), VatM (N2, Dr. R. Allen (Fok, Clarke et al. 1993)), mitochondrial porin (Dr. G. Gerisch), p80 (purchased from the Geneva Antibody Facility), cocktail *M. leprae* MLSA, MLMA and MLcwA, calreticulin (mAb, 251-67-1) (gift of Dr. G. Gerisch, MPI for Biochemistry, Martinsried), PDI. Goat anti-mouse or anti-rabbit IgG coupled to AlexaFluor594 (Invitrogen) were used as secondary antibodies.

EM

Cells were fixed and stained as previously described (Barisch et al., 2015). Cells were fixed for 1 h in 2% glutaraldehyde and then, stained for 30 min in a 2% osmium/0.1 M imidazole solution. After 2 washes in PBS, cells were then sent to the EM platform of the Faculty of Medicine, University of Geneva, where the samples were fixed, embedded in Epon resin and processed for EM. Grids were observed with a Tecnai 20 electron microscope (FEI).

Isolation of MCV

At time of interest (1, 3 or 6 hpi), the infection was stopped by pelleting the infected cells at 4°C for 8 min at 2000 rpm. Cells were resuspended in cold HESES-azide buffer (20 mM HEPES-KOH, 0.25 M sucrose, 5 mM azide, pH 7.2) containing a protease-inhibitor cocktail (Complete EDTA-free, Roche) and homogenized by passing them 8 times through a ball homogenizer (HGM, Germany) with a 10 µm clearance. The cell homogenate was then incubated with 10 mM Mg-ATP on a rotating wheel for 15 min at 4°C and loaded onto sucrose step gradients (layers of 10%, 30%, 40% and 60% sucrose). After overnight ultracentrifugation of the gradients at 28 000 rpm in a SW40 rotor at 4°C, MCVs were collected at the 10-30% sucrose interphase and diluted in membrane buffer (20 m*M* HEPES-KOH, pH 7.2, 20 m*M* KCl, 2.5 m*M* MgCl2, 1 m*M* dithiothreitol (DTT), 20 m*M* NaCl). MCVs were then pelleted by ultracentrifugation for 1h30 at 35 000 rpm at 4°C in a SW40 rotor. Dry pellets of MCV were finally snap-frozen and stored at -80°C until further analysis.

Samples reduction, alkylation, digestion and TMT labelling

The reduction, alkylation, digestion and TMT labelling were mainly performed as described by (Dayon, Hainard et al. 2008). Briefly, the MCV pellets were resuspended in 50 µL of TEAB (Triethylammonium hydrogen carbonate buffer) 0.1 M pH 8.5, 6 M urea. After addition of 50 mM of TCEP (tris-(2-carboxyethyl) phosphine hydrochloride), reduction was performed during 1 h at 37°C. The samples were then centrifuged several times for 10 min, at 12,000 rpm until the collected supernatants were completely free of latex beads. Protein concentration of each sample was measured with the help of a nanodrop. 100 µg of proteins of each sample were alkylated at RT in the dark for 30 min. after addition of 1 µL of IAA (Iodoacetamide) 400 mM. The volume of the samples was then adjusted to 100 µL with TEAB 0.1 M pH 8.5. After addition of 2 µg of trypsin, samples were digested overnight at 37°C. Each sample was then labelled with one TMT reagent according to manufacturer's instructions. Finally, 50 µL of each labelled sample were pooled and evaporated under speed-vacuum.

OGE

Off-gel electrophoresis was performed according to manufacturer's instructions (Agilent). After desalting, the mix containing the pooled labelled samples was reconstituted in OFFGEL solution. A 12 or 24-wells frame was set-up on an Immobiline DryStrip pH 3-10, 24 cm and isoelectric focusing was performed with those settings: 8,000 V, 50 µA, 200 mW until 20 kVh was reached. The fractions were then recovered and desalted using C18 MicroSpin columns.

Mass spectrometry

ESI LTQ-OT MS was performed on an LTQ Orbitrap Velos from Thermo Electron (San Jose, CA, USA) equipped with a NanoAcquity system from Waters. Peptides were trapped on a home-made 5 µm 200 Å Magic C18 AQ (Michrom) 0.1 × 20 mm pre-column and separated on a home-made 5 µm 100 Å Magic C18 AQ (Michrom) 0.75 × 150 mm column with a gravity-pulled emitter. The analytical separation was run for 65 min using a gradient of H2O/FA 99.9%/0.1% (solvent A) and CH3CN/FA 99.9%/0.1% (solvent B). The gradient ran as follows: 0–1 min 95% A and 5% B, then to 65% A and 61 35% B at 55 min, and 20% A and 80% B at 65 min at a flow rate of 220 nL/min. For MS survey scans, the OT resolution was set to 60000 and the ion population was set to 5 × 105 with an m/z window from 400 to 2000. A maximum of 3 precursors was selected for both collision-induced dissociation (CID) in the LTQ and high-energy C-trap dissociation (HCD) with analysis in the OT. For MS/MS in the LTQ, the ion population was set to 7000 (isolation width of 2 m/z) while for MS/MS detection in the OT, it was set to 2 × 10E5 (isolation width of 2.5 m/z), with resolution of 7500, first mass at m/z = 100, and maximum injection time of 750 ms. The normalized collision energies were set to 35% for CID and 60% for HCD.

Protein identification

Protein identification was performed with the help of the Easyprot platform. The Easyprot platform proceeds as

follows: peak lists are generated from raw data using (ReadW). After peaklist generation, the CID and HCD spectra are merged for simultaneous identification and quantification (Dayon, Pasquarello et al. 2010 and http://www.expasy.org/tools/HCD_CID_merger.html).
The peaklist files were searched against the uniprot_sprot database (2011_02 of 08-Feb-2011). *Dictyostelium discoideum*, *Mycobacterium marinum* and *Mycobacterium smegmatis* taxonomies were specified for database searching. The parent ion tolerance was set to 10 ppm. TMT-sixplex amino terminus, TMT-sixplex lysine (229.1629 Da) and carbamidomethylation of cysteines were set as fixed modifications. Oxidized methionine was set as variable amino acid modification. Trypsin was selected as the enzyme, with one potential missed cleavage, and the normal cleavage mode was used. Protein and peptide scores were then set up to maintain the false positive peptide ratio below 1%. For identification, only proteins matching two different peptide sequences were kept.

Protein quantification

Isobaric quantification was performed using the IsoQuant module of Easyprot's protein export as described previously. Briefly, a false discovery rate of 1% and a minimum of 2 peptides per protein were selected. TMT sixplex was selected as reporter and a mass tolerance of 0.05 m/z was used. The different protein ratios were calculated. A global normalisation of "median log peptide ratio=0" and a confidence threshold of 95% were selected. EasyProt's Mascat statistical method, inspired by Mascot's quantification module (http://www.matrixscience.com/help/quant_statistics_help.html), and Libra, inspired by the Trans-Proteomic Pipeline's isobaric quantification module (http://tools.proteomecenter.org/wiki/index.php?title=Software:Libra), were chosen, along the generation of the list of proteins featuring a ratio fold over 1.5. To determine the proteins differentially abundant, a cutoff threshold was calculated for each sample comparison as described previously. The results of those calculations are presented in **Table S5**.

REFERENCES

Arafah, S., S. Kicka, V. Trofimov, M. Hagedorn, N. Andreu, S. Wiles, B. Robertson and T. Soldati (2013). Setting up and monitoring an infection of Dictyostelium discoideum with mycobacteria. Dictyostelium Protocols (Methods Mol Bio). L. Eichinger and F. Rivero, Humana Press. **983:** 403-417.

Barisch, C., P. Paschke, M. Hagedorn, M. Maniak and T. Soldati (2015). "Lipid Droplet Dynamics at Early Stages of Mycobacterium marinum Infection in Dictyostelium." Cell Microbiol **17**(9): 1332-1349.

Barisch, C. and T. Soldati (2017). "Mycobacterium marinum Degrades Both Triacylglycerols and Phospholipids from Its Dictyostelium Host to Synthesise Its Own Triacylglycerols and Generate Lipid Inclusions." PLoS Pathog **13**(1): e1006095.

Benghezal, M., M. O. Fauvarque, R. Tournebize, R. Froquet, A. Marchetti, E. Bergeret, B. Lardy, G. Klein, P. Sansonetti, S. J. Charette and P. Cosson (2006). "Specific host genes required for the killing of Klebsiella bacteria by phagocytes." Cell Microbiol **8**(1): 139-148.

Buckley, C. M., N. Gopaldass, C. Bosmani, S. A. Johnston, T. Soldati, R. H. Insall and J. S. King (2016). "WASH drives early recycling from macropinosomes and phagosomes to maintain surface phagocytic receptors." Proc Natl Acad Sci U S A **113**(40): E5906-E5915.

Cardenal-Munoz, E., S. Arafah, A. T. Lopez-Jimenez, S. Kicka, A. Falaise, F. Bach, O. Schaad, J. S. King, M. Hagedorn and T. Soldati (2017). "Mycobacterium marinum antagonistically induces an autophagic response while repressing the autophagic flux in a TORC1- and ESX-1-dependent manner." PLoS Pathog **13**(4): e1006344.

Clarke, M., J. Kohler, Q. Arana, T. Liu, J. Heuser and G. Gerisch (2002). "Dynamics of the vacuolar H(+)-ATPase in the contractile vacuole complex and the endosomal pathway of Dictyostelium cells." J Cell Sci **115**(Pt 14): 2893-2905.

Dieckmann, R., A. Gueho, R. Monroy, T. Ruppert, G. Bloomfield and T. Soldati (2012). "The balance in the delivery of ER components and the vacuolar proton pump to the phagosome depends on myosin IK in Dictyostelium." Mol Cell Proteomics **11**(10): 886-900.

Fok, A. K., M. Clarke, L. Ma and R. D. Allen (1993). "Vacuolar H-ATPase of Dictyostelium Discoideum: A monoclonal antibody study." J Cell Sci. **106**: 1103-1113.

Hagedorn, M., E. N. Neuhaus and T. Soldati (2006). "Optimised fixation and immunofluorescence protocols for Dictyostelium cells." Methods Mol. Biol. **Dictyostelium discoideum Protocols edited by Eichinger and Rivero, Humana Press Totowa, NJ.** : Chapter 20:327-338.

Hagedorn, M. and T. Soldati (2007). "Flotillin and RacH modulate the intracellular immunity of Dictyostelium to Mycobacterium marinum infection." Cell Microbiol **9**(11): 2716-2733.

Jenne, N., R. Rauchenberger, U. Hacker, T. Kast and M. Maniak (1998). "Targeted gene disruption reveals a role for vacuolin B in the late endocytic pathway and exocytosis." J Cell Sci **111 (Pt 1)**: 61-70.

Journet, A., G. Klein, S. Brugiere, Y. Vandenbrouck, A. Chapel, S. Kieffer, C. Bruley, C. Masselon and L. Aubry (2012). "Investigating the macropinocytic proteome of Dictyostelium amoebae by high-resolution mass spectrometry." Proteomics **12**(2): 241-245.

Kolonko, M., A. C. Geffken, T. Blumer, K. Hagens, U. E. Schaible and M. Hagedorn (2014). "WASH-driven actin polymerization is required for efficient mycobacterial phagosome maturation arrest." Cell Microbiol **16**(2): 232-246.

Le Coadic, M., R. Froquet, W. C. Lima, M. Dias, A. Marchetti and P. Cosson (2013). "Phg1/TM9 proteins control intracellular killing of bacteria by determining cellular levels of the Kil1 sulfotransferase in Dictyostelium." PLoS One **8**(1): e53259.

Lopez-Jimenez, A. T., E. Cardenal-Munoz, F. Leuba, L. Gerstenmaier, C. Barisch, M. Hagedorn, J. S. King and T. Soldati (2018). "The ESCRT and autophagy machineries cooperate to repair ESX-1-dependent damage at the Mycobacterium-containing vacuole but have opposite impact on containing the infection." PLoS Pathog **14**(12): e1007501.

Sattler, N., C. Bosmani, C. Barisch, A. Gueho, N. Gopaldass, M. Dias, F. Leuba, F. Bruckert, P. Cosson and T. Soldati (2018). "Functions of the Dictyostelium LIMP-2 and CD36 homologues in bacteria uptake, phagolysosome biogenesis and host cell defence." J Cell Sci **131**(17).

Sattler, N., R. Monroy and T. Soldati (2013). "Quantitative analysis of phagocytosis and phagosome maturation." Methods Mol Biol **983**: 383-402.

FIGURE LEGENDS

Figure 1. BBCs are recognized and phagocytosed as mycobacteria by *D. discoideum*. A. Experimental strategy used to isolate mycobacteria-containing vacuoles (MCVs) from infected cells. Latex beads were adsorbed onto mycobacteria. A pure inoculum of bacteria and bead complexes (BBCs) was prepared and used to infect *D. dictyostelium* cells. At times of interest, cells were homogenized, and the homogenate was loaded onto a sucrose gradient and ultracentrifuged. Compartments containing BBCs float at the top of the sucrose gradient and were recovered. **B**. *M. marinum*-GFP-BBCs prepared with 0.2 µm latex beads. For ease of visualisation, TRITC-coupled antibodies (red) were adsorbed onto latex beads during BBCs preparation. Scale bar, 1 µm. **C**. Wild type cells were infected with *M. marinum*-GFP or *M. marinum*-GFP-BBCs prepared with different sizes of latex beads. The proportion of infected cells was determined by FACS. The values were normalized to the number of infected cells obtained for the infection performed with non-coated *M. marinum*-GFP. Bars represent mean and SD of 4 independent experiments (one-way ANOVA, **p<0.01). **D**. BBCs were prepared with *M. marinum*-GFP and 0.2 µm latex beads and stained for anti-mycobacterial cell wall material with a cocktail of antibodies (anti-*M. leprae* membrane antigens, anti-*M. leprae* surface antigens, anti-*M. leprae* cell wall associated antigens, red). Scale bars, 2 µm. **E**. The uptake of non-coated *M. marinum*-GFP (right) and of 0.2 µm-*M. marinum*-GFP-BBCs (left) by wild type and *lmpB*-ko cells was measured by FACS. Relative fluorescence was normalized to the value obtained for wild type cells at 90 min. The curve represents the mean and SD of 3 independent experiments. **F**. Wild type cells were infected with 0.2 µm-*M. marinum*-GFP-BBCs. At 21 hpi, cells were immunostained against p80 or vacuolin. Arrowheads indicate p80- or vacuolin-positive membranes around *M. marinum*-BBCs. Scale bar, 10 µm. **G**. Wild type cells were infected with 0.2 µm-*M. marinum*-GFP-BBCs. At 21 hpi, cells were processed for Transmission Electron Microscopy (TEM). Arrowheads indicate 0.2 µm latex beads.

Figure 2. BBCs are infectious and behave as non-coated mycobacteria. A. Wild type cells were infected with *M. smegmatis*-GFP, *M. marinum*-L1D-GFP, *M. marinum*-GFP or BBCs prepared with these different strains. After removing uningested bacteria or BBCs, infection was monitored by FACS. Representative SSC (side scatter) vs FL-1 (GFP fluorescence) plots are presented. Three different populations can be distinguished, as represented on the right panel: non-infected cells (red), infected cells (black) and extracellular mycobacteria or BBCs (green). **B**. Wild type cells were infected with *M. marinum*-lux. Intracellular mycobacteria growth was monitored by measuring the luminescence at indicated times. The curves represent the mean fold increase of luminescence and SD of 3 independent experiments. **C**. Wild type cells were infected with 0.2 µm-*M. marinum*-GFP-BBCs. At 21 hpi, cells were processed for TEM. Arrowheads indicate 0.2 µm latex beads.

Figure 3. Vacuoles containing different mycobacteria strains can be isolated. A. Wild type cells were infected with 0.2 µm-*M. marinum*-GFP-BBCs. At 1 hpi, cells were homogenized. After incubation with ATP, the cell homogenate was ultracentrifuged on a sucrose gradient. The fraction recovered at the 10 %-30 % interphase was observed by microscopy. Scale bar, 10 µm; in the zoom-in, 2 µm. **B**. MCVs containing 0.2 µm-BBCs prepared with *M. marinum*-GFP, *M. marinum*-L1D or *M. smegmatis* were isolated from wild type cells and immunostained against p80, VatM or vacuolin. The number of compartments positive for the different markers were counted for each mycobacteria strain. Scale bars, 1 µm. Graphs represent mean and SEM of 2 independent experiments. **C**. MCVs containing 0.2 µm-*M. marinum*-GFP-BBCs were isolated from wild type cells and immunostained against PDI, calreticulin or mitochondrial porin (red). Scale bars, 10 µm.

Figure 4. Proteomic analysis of the *M. marinum*-MCV during the early phase of infection (1 to 6 hpi). *M. marinum*-MCV were isolated at 1, 3 and 6 hpi. After labelling with TMT, equal amounts of each sample were mixed. This pool was analysed by LC-MS/MS. **A**. Vien diagram depicting the number of proteins commonly found in the *M. marinum*-MCV proteome and in the published phagosome proteome, and macropinosome proteome. **B.** Functional classification of the 1606 *D. discoideum* proteins identified in the *M. marinum*-MCV proteome by mass spectrometry. As a comparison, results from a previous phagosome proteome analysis are also presented, and classified using the same classification terms. Percentages of identified proteins in the different classes are indicated. **C.** Functionnal clustering of the *M. marinum*-MCV proteome with the help of the DAVID functional annotation clustering tool. The default parameters of the program were used and the categories Gene Ontology "biological process" and KEGG were selected. Enriched GO-terms are presented according to their enrichment score and p-value. Size of the bubble represents the number of

proteins in the cluster. Color indicates GO-terms belonging to the same cluster.

Figure 5. Temporal modification of the *M. marinum*-MCV during the early phase of infection (1 to 6 hpi) *M. marinum*-MCV were isolated at 1, 3 hpi and 6 hpi. After labelling with TMT, equal amounts of each sample were mixed. This pool was analysed and quantified by LC-MS/MS. Both *M. marinum*-MCV isolated at 3 and 6 hpi were compared to *M. marinum*-MCV isolated at 1 hpi. For each identified protein, the protein ratios of the corresponding comparison were calculated. **A.** Ratios of the 232 *D. discoideum* MCV proteins significantly differentially abundant during the early phase of infection. Ratios no significantly different from 1 were noted as 1. **B.** MCV proteins significantly differentially abundant during the early phase of infection were functionally classified using the same classification terms as in Figure 4. *M. marinum*-MCV proteins significantly depleted at 3 hpi **(C)**, at 6 hpi **(D)** or accumulating at 6 hpi **(E)** were functionally clustered using the DAVID functional annotation clustering tool (Huang et al., 2009a; Huang et al., 2009b). The default parameters of the program were used and the categorie Gene Ontology "biological process" was selected. Enriched GO-terms are presented according to their enrichment score and p-value. Size of the bubble represents the number of proteins in the cluster. Color indicates GO-terms belonging to the same cluster.

Figure 6. *M. marinum* MCV comparison with non-manipulated Mycobacterium-containing compartments. MCVs containing *M. marinum*, *M. marinum*-L1D, *M. smegmatis* or *M. marinum*-RD1 were isolated at 1 and 6 hpi. All samples were labelled with TMT. *M. marinum*-MCVs were mixed with equal amounts of each other mycobacteria-MCVs. The obtained pools were analysed and quantified by LC-MS/MS. For each identified protein, the protein ratios of the corresponding comparison were calculated. The numbers of significantly differentially abundant proteins for each comparison are summarized in the table.

Figure S1. Latex beads adsorb onto Mycobacteria and can float them up on a sucrose gradient. A. *M. marinum*-GFP-BBCs were prepared with latex beads of different sizes and various beads:bacteria ratios. The resulting BBCs were visualized by microscopy. **B**. *M. marinum*-GFP-BBCs prepared with different latex bead sizes. TRITC-coupled antibodies were adsorbed onto latex beads during BBCs preparation. Scale bar, 1 µm. **C**. *M. marinum*-GFP-BBCs were prepared with 0.8 µm or0.5 µm latex beads at ratios 15 and 90 respectively. The prepared BBCs+free beads mixture was loaded onto a sucrose gradient. Fractions recovered at the different interphases were visualized by microscopy. **D**. *M. marinum*-GFP-BBCs prepared with 0.8 µm, 0.5 µm or 0.2 µm latex beads at ratios 15, 90 and 500 respectively and separated from free beads by ultracentrifugation on a one step sucrose gradient were loaded on the sucrose gradient used to isolate latex-bead phagosomes. The majority of the BBCs float at the 10%-25% interphase.

Table S1. *M. marinum*-MCV early proteome

Table S2. *M. marinum*-MCV early proteome KEGG pathways

Table S3. Proteins differentially abundant during *M. marinum*-MCV establishment

Table S4. Proteins differentially abundant in M. marinum-MCV compared to non or less-manipulated MCVs

Table S5. MS thresholds calculations

Figure 1

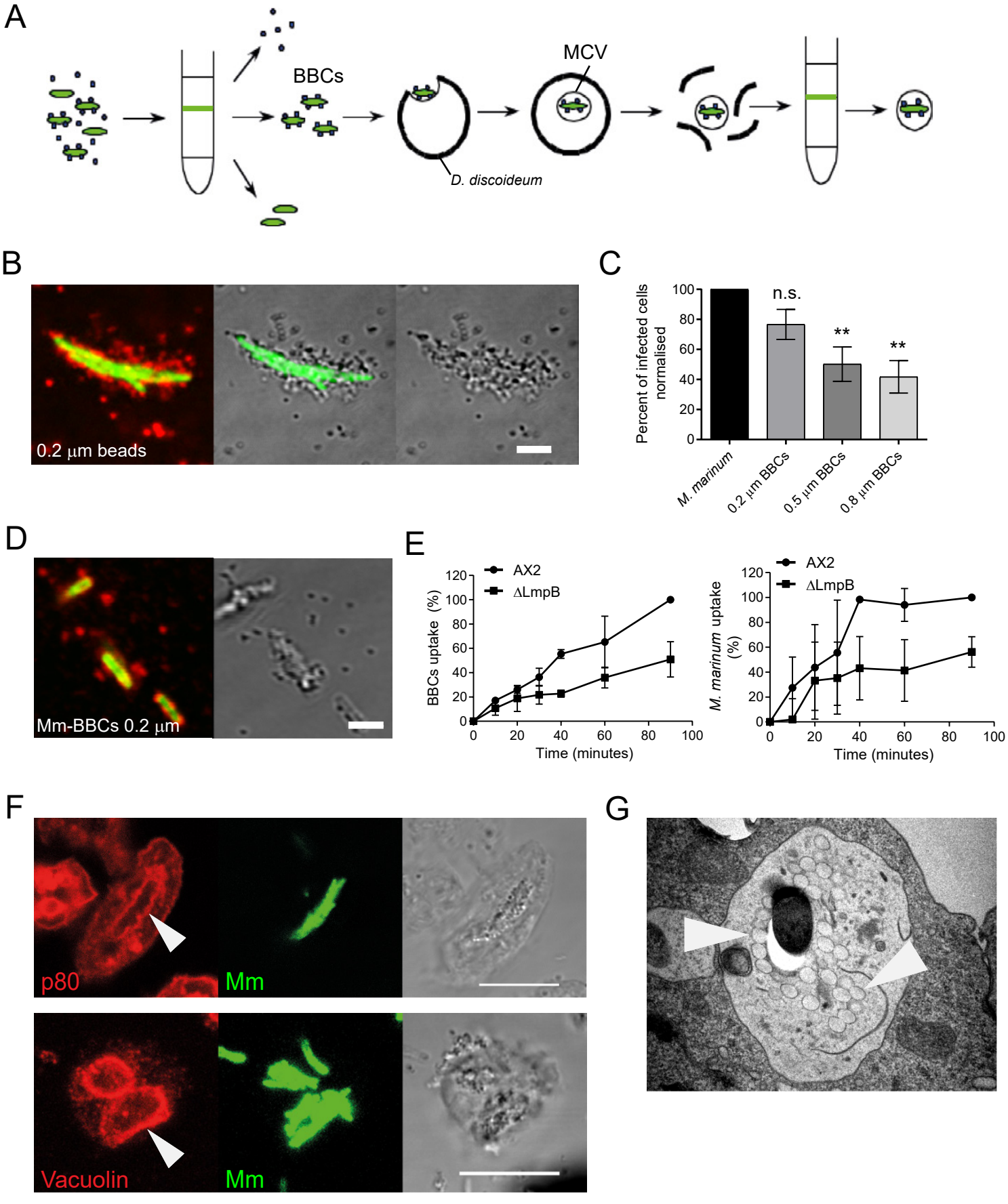

Guého et al.,

Figure 2

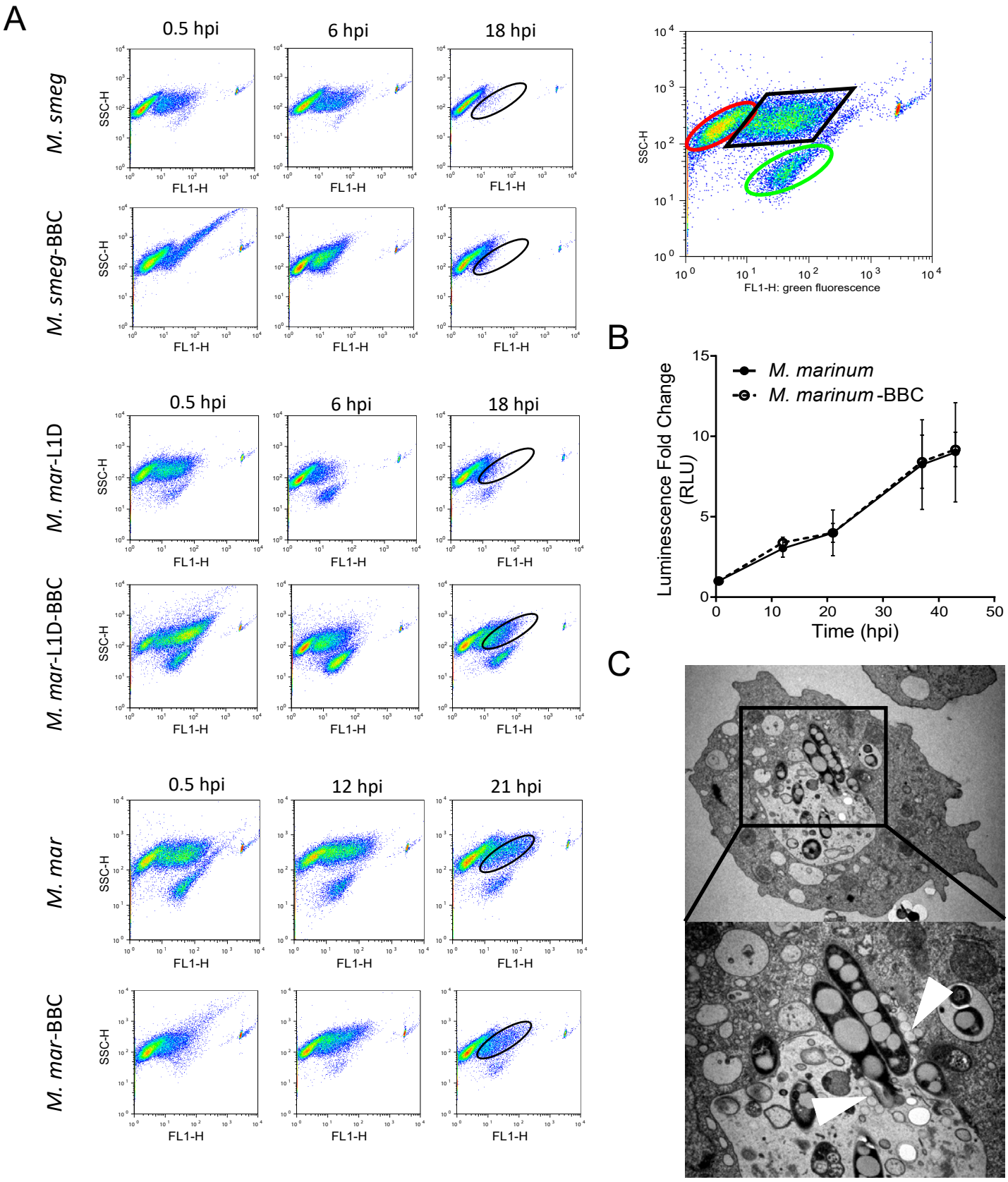

Guého et al.,

Figure 3

A

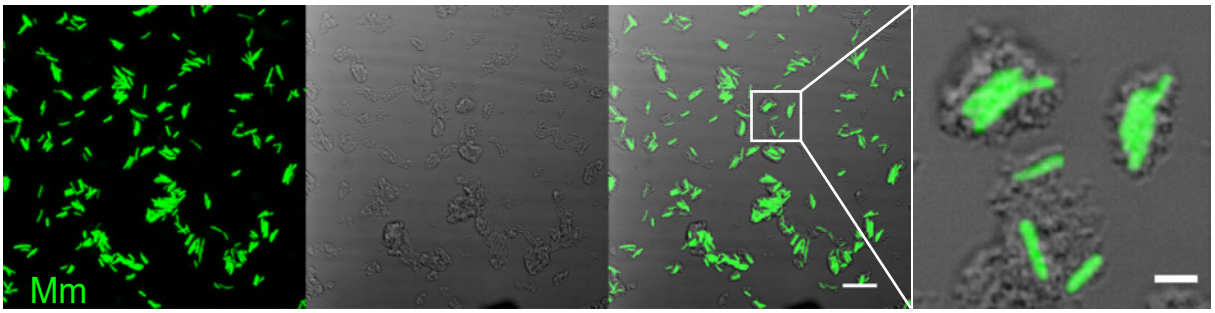

B

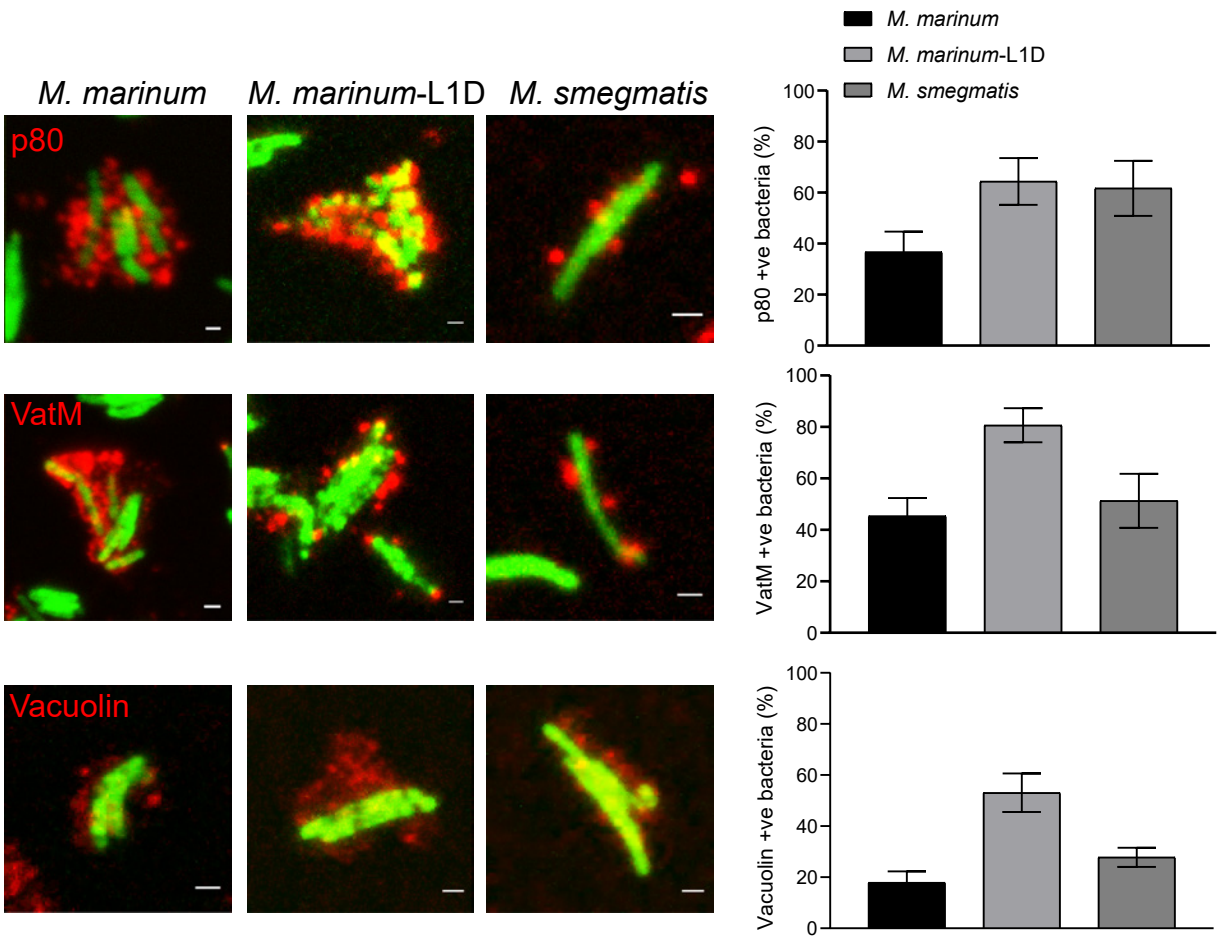

C

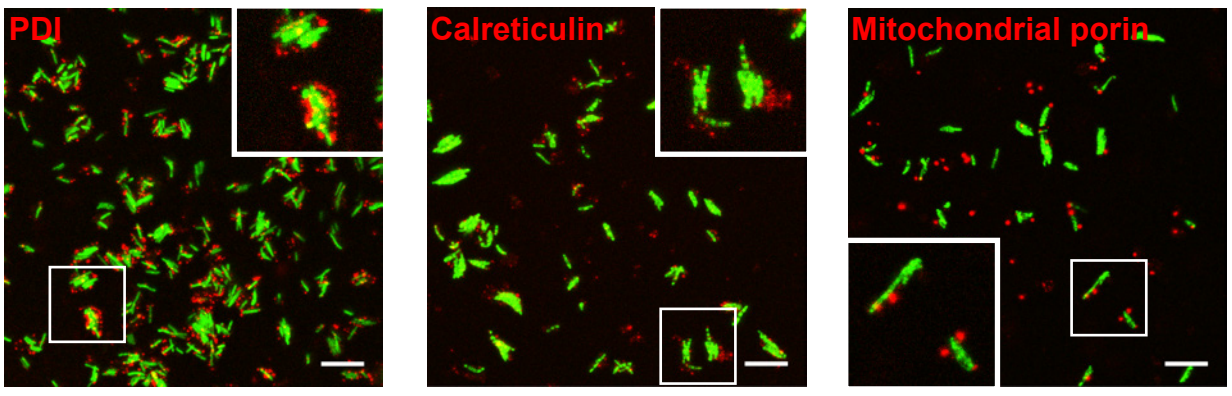

Figure 4

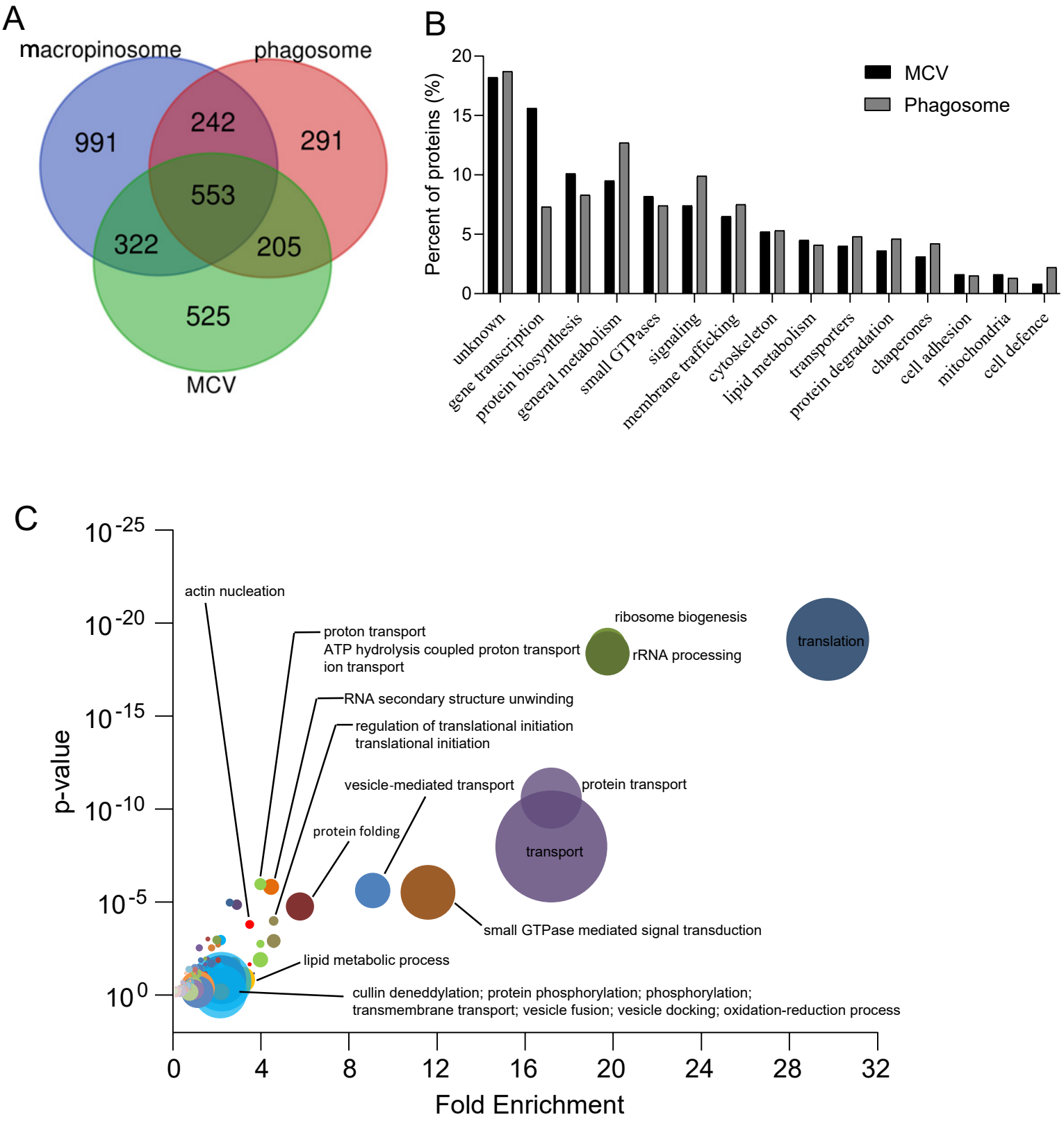

Figure 5

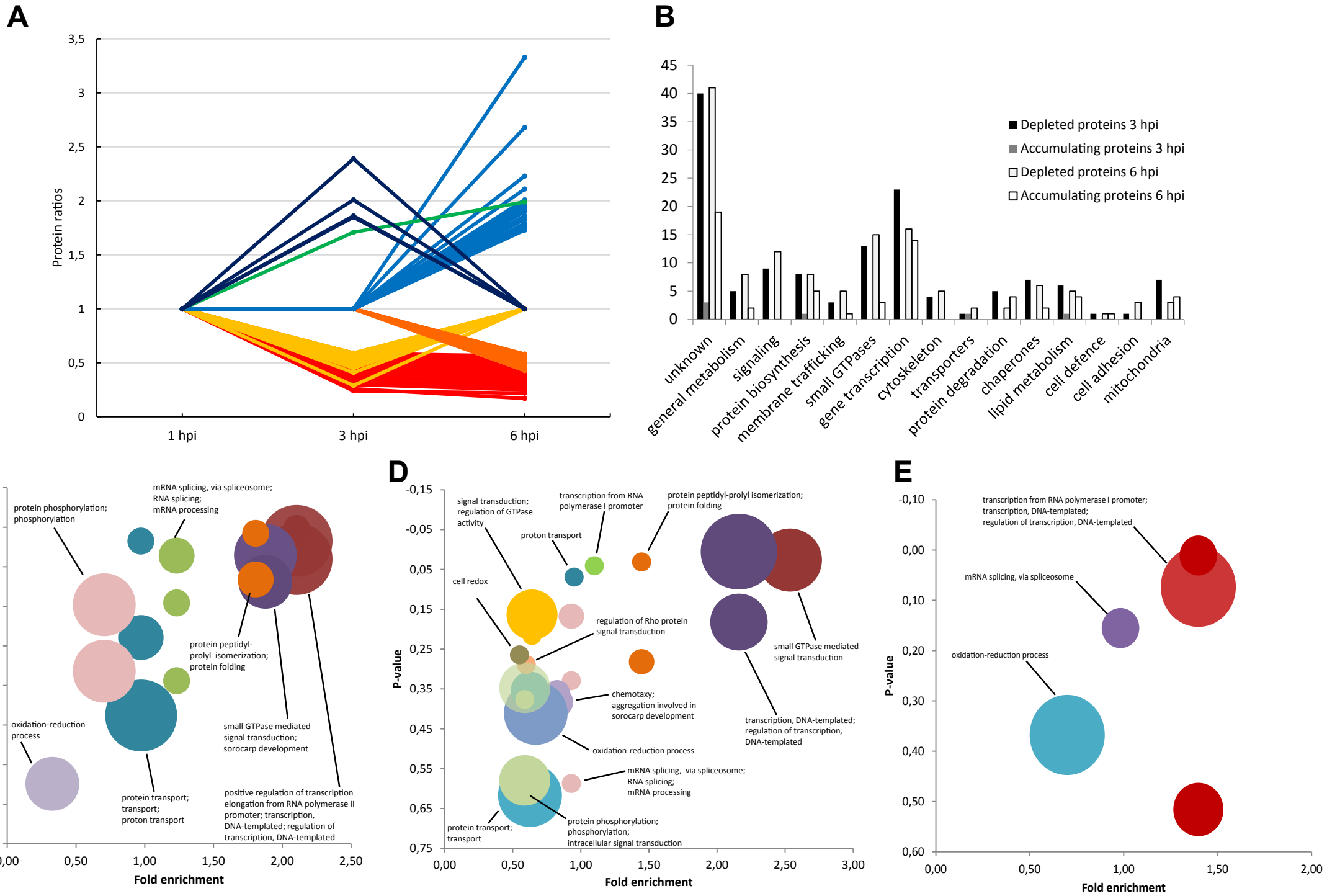
A
Protein ratios
1 hpi
3 hpi
6 hpi
B
Depleted proteins 3 hpi
Accumulating proteins 3 hpi
Depleted proteins 6 hpi
Accumulating proteins 6 hpi
unknown
general metabolism
signaling
protein biosynthesis
membrane trafficking
small GTPases
gene transcription
cytoskeleton
transporters
protein degradation
chaperones
lipid metabolism
cell defence
cell adhesion
mitochondria
C
P-value
Fold enrichment
protein phosphorylation; phosphorylation
mRNA splicing, via spliceosome; RNA splicing; mRNA processing
protein peptidyl-prolyl isomerization; protein folding
oxidation-reduction process
small GTPase mediated signal transduction; sorocarp development
protein transport; transport; proton transport
positive regulation of transcription elongation from RNA polymerase II promoter; transcription, DNA-templated; regulation of transcription, DNA-templated
D
P-value
Fold enrichment
signal transduction; regulation of GTPase activity
transcription from RNA polymerase I promoter
protein peptidyl-prolyl isomerization; protein folding
proton transport
cell redox
regulation of Rho protein signal transduction
small GTPase mediated signal transduction
chemotaxy; aggregation involved in sorocarp development
transcription, DNA-templated; regulation of transcription, DNA-templated
oxidation-reduction process
mRNA splicing, via spliceosome; RNA splicing; mRNA processing
protein transport; transport
protein phosphorylation; phosphorylation; intracellular signal transduction
E
P-value
Fold enrichment
transcription from RNA polymerase I promoter; transcription, DNA-templated; regulation of transcription, DNA-templated
mRNA splicing, via spliceosome
oxidation-reduction process

Figure 6

***M. marinum* -MCV compared to**	**1 hpi**		**6 hpi**	
	Enriched	**Depleted**	**Enriched**	**Depleted**
***M. marinum* -L1D MCV**	13	48	Not done	Not done
***M. smegmatis* -MCV**	11	49	69	0
***M. marinum-RD1* -MCV**	63	22	111	25

Guého et al.,

Figure S1